Six low-strain zinc-blende half metals: An *ab initio* investigation

J. E. Pask,[1,*] L. H. Yang,[1] C. Y. Fong,[2] W. E. Pickett,[2] and S. Dag[3]
[1]*H-Division, Lawrence Livermore National Laboratory, Livermore, California 94551, USA*
[2]*Department of Physics, University of California, Davis, California 95616, USA*
[3]*Department of Physics, Bilkent University, Ankara, Turkey*
(Received 17 January 2003; published 17 June 2003)

A class of spintronic materials, the zinc-blende (ZB) half metals, has recently been synthesized in thin-film form. We apply all-electron and pseudopotential *ab initio* methods to investigate the electronic and structural properties of ZB Mn and Cr pnictides and carbides, and find six compounds to be half metallic at or near their respective equilibrium lattice constants, making them excellent candidates for growth at low strain. Based on these findings, we further propose substrates on which the growth may be accomplished with minimum strain. Our findings are supported by the recent successful synthesis of ZB CrAs on GaAs and ZB CrSb on GaSb, where our predicted equilibrium lattice constants are within 0.5% of the lattice constants of the substrates on which the growth was accomplished. We confirm previous theoretical results for ZB MnAs, but find ZB MnSb to be half metallic at its equilibrium lattice constant, whereas previous work has found it to be only nearly so. We report here two low-strain half metallic ZB compounds, CrP and MnC, and suggest appropriate substrates for each. Unlike the other five compounds, we predict ZB MnC to become/remain half metallic with compression rather than expansion, and to exhibit metallicity in the minority- rather than majority-spin channel. These fundamentally different properties of MnC can be connected to substantially greater *p-d* hybridization and *d-d* overlap, and correspondingly larger bonding-antibonding splitting and smaller exchange splitting. We examine the relative stability of each of the six ZB compounds against NiAs and MnP structures, and find stabilities for the compounds not yet grown comparable to those already grown.

DOI: 10.1103/PhysRevB.67.224420 PACS number(s): 75.50.Cc, 71.20.Be

I. INTRODUCTION

Spintronic devices, which exploit the spin of electrons as well as their charge, have already yielded breakthroughs in information storage and hold the promise of doing the same for memory, microprocessors, and a host of other technologies.[1–4] In spintronic applications, materials containing atoms having large atomic magnetic moments ($>1\mu_B$, where μ_B is the Bohr magneton) and high Curie temperatures (above room temperature) are critical. One class of materials which has been successfully employed in spintronic applications is the magnetically doped semiconductors.[5–8] These materials can exhibit atomic moments in excess of $3\mu_B$ per magnetic atom. However, because of the doping, incoherence of carrier transport is an issue in device performance. Furthermore, the most studied doped cubic semiconductor, Mn-doped GaAs, suffers from a low Curie temperature $T_C=110$ K.

Another class of materials which has been considered for spintronic applications is the half metals (HMs).[9] de Groot *et al.*[10] were the first to introduce the term ''half metal'' in studying the $C1_b$-type Heusler alloys, NiMnSb and PtMnSb. Half metals are so named because one spin channel is metallic while the other is insulating. The polarization of the carriers is thus complete, contributed entirely by one spin channel at the Fermi energy, E_F. This is in marked contrast to the usual ferromagnetic metals such as iron in which both spin channels contribute at E_F, resulting in substantially less than 100% polarization. Because of the complete polarization in HMs, layered structures in which they are incorporated can exhibit large magnetoresistances, and so show great promise for a variety of device applications.[9] In addition to the Heusler alloys, some transition-metal oxides have been found to be ferromagnetic and half metallic, for example, perovskites[11] and rutile structured CrO_2.[12–14] However, the stoichiometry of these compounds has proven difficult to control[15] and defects limit coherent transport that is essential for most spintronic applications.

The complications associated with the aforementioned compounds motivated Akinaga *et al.*[16] to search for HMs with simple structures, large magnetic moments, and high Curie temperatures. They found zinc-blende (ZB) CrAs to be half metallic in full-potential linearized augmented plane-wave (LAPW) calculations, and subsequently succeeded in growing this compound in thin-film form (2.0 nm). Experimentally, they found a $T_C>400$ K, and a magnetic moment of $3\mu_B$ per f.u., consistent with *ab initio* predictions. Subsequently, the synthesis of monolayer CrSb on GaSb, (Ga,Al)Sb, and GaAs substrates was reported.[17] These compounds are half metallic, and have large magnetic moments, high T_C (above room temperature), and a simple ZB structure. They are thus promising for device applications involving existing III-V semiconductor technologies.

Since the initial prediction and subsequent synthesis of ZB CrAs,[16] several theoretical studies on this class of compounds have appeared,[18–29] employing a number of *ab initio* methods: plane-wave pseudopotential (PWPP),[21] LAPW,[16,18,20,24,25,28] linear muffin-tin orbital,[19,29] full-potential screened Korringa-Kohn-Rostoker, [26,27] and atomiclike orbital.[22,25] Issues addressed in these studies include the existence of half metallicity at different lattice constants,[21,24,27,28] with different surface terminations,[26,27] in the context of interfaces,[23] and under different exchange-correlation approximations;[24,28] stability of ferromagnetic ZB relative to other crystal and magnetic structures,[20,21,23–25] the nature of the magnetism in ZB vs other crystal

structures,[18,24,25] the effect of cation[20] and anion[24] species on magnetism, the nature of the bonding,[21,22,24,26–28] the induced antiparallel moment of the anion,[18,19,22] the stability of ferromagnetism with temperature,[29] and the effectiveness of all-electron generalized gradient approximation (GGA) *ab initio* methods relative to the use of pseudopotentials and/or the local-density approximation (LDA).[24,25]

In this work, we apply both all-electron and pseudopotential *ab initio* methods to investigate the electronic and structural properties of Mn and Cr pnictides and carbides, and find six compounds to be half metallic at or near their respective equilibrium lattice constants, making them excellent candidates for growth at low strain. Based on these findings, we further propose substrates on which the growth may be accomplished with minimum strain. We confirm previous theoretical results for ZB MnAs, but find ZB MnSb to be half metallic at its equilibrium lattice constant, whereas previous work has found it to be only nearly so. In addition, we find two ZB compounds, CrP and MnC, to be half metallic near their respective equilibrium lattice constants, and suggest appropriate substrates for each. While ZB Cr and Mn pnictides are well suited to integration with existing III-V semiconductor technologies, ZB MnC may be particularly well suited to integration into either diamond or cubic (β-phase) SiC technologies, and so may be an excellent candidate for spintronics in high-pressure environments, and possibly high-temperature applications. We examine the bonding in these materials in some detail, and explain the fundamental differences between the half metallicity of MnC and the other five.

In Sec. II, we discuss the computational methods employed in this work. In Sec. III, we discuss the predicted half metallic compounds and appropriate substrates, with particular attention to the bonding in these materials, and differences between MnC and the rest. We summarize in Sec. IV.

II. METHODS OF CALCULATION

To clarify some questions that have arisen in previous work, we employed both pseudopotential and all-electron *ab initio* density-functional methods.[30] An ultrasoft PWPP method[31–34] was used for all calculations, and all-electron full-potential LAPW calculations[35,36] were performed to determine equilibrium lattice constants, half metallic lattice constants, magnetic moments, and densities of states, as a check on the pseudopotential results. Where both methods were employed, both results are reported to demonstrate the excellent agreement of the two. This is significant since it demonstrates that a pseudopotential approach is viable for such calculations, contrary to an earlier report based on a different pseudopotential method,[25] and so opens the way for much larger calculations than are practical with full-potential all-electron approaches.

In the pseudopotential calculations, a GGA functional[37] for exchange and correlation was employed. A plane-wave cutoff of 450 eV and Brillouin-zone sampling of 3375 k points (corresponding to 120 points in the irreducible wedge) were used in all ZB calculations. Increasing the plane-wave cutoff from 450 eV to 650 eV, and changing the k-point sampling from 1331 to 3375 to 4913 points in the full zone, yielded changes in total energy of less than 1 meV per f.u. in all cases. The same plane-wave cutoff was used for the NiAs and MnP structures as for the ZB structures. For NiAs structures, the c/a ratio was optimized; for MnP structures, both c/a and b/a were optimized.

TABLE I. Six ZB Cr and Mn pnictide and carbide compounds that exhibit half metallicity at or near their respective equilibrium lattice constants. For each compound, the equilibrium lattice constant a_0, half metallic lattice constant a_{HM} (lattice constant nearest equilibrium at which half metallicity is predicted), DOS at E_F, insulating-channel gap, and magnetic moment per formula unit are given. For each compound, LAPW results are listed on first lines, PWPP results on second lines.

Compound	a_0 (Å)	a_{HM} (Å)	DOS at E_F (states/eV spin)	Gap (eV)	Moment (μ_B)
CrP	5.35	5.48	0.85	1.88	3.0
	5.42	5.47	0.82	1.86	3.0
CrAs	5.67	5.67	0.85	1.88	3.0
	5.66	5.66	0.85	1.85	3.0
CrSb	6.15	6.15	0.90	1.58	3.0
	6.14	6.14	0.87	1.54	3.0
MnAs	5.72	5.75	0.76	1.74	4.0
	5.74	5.77	0.77	1.70	4.0
MnSb	6.19	6.19	0.78	1.41	4.0
	6.21	6.21	0.79	1.40	4.0
MnC	4.36	4.26	1.23	0.79	1.0
	4.39	4.20	1.24	0.90	1.0

In the LAPW calculations, a GGA functional[38] for exchange and correlation was also employed. A cutoff of $RK_{max}=8$ was used in the representation of the wave functions, $G_{max}=16$ a.u.$^{-1}$ for the charge density, and 4096 k points were used to sample the Brillouin zone. Convergence with respect to basis set and k-point sampling was carefully verified. The effects of different core-valence energy partitions and local orbitals were also checked.

III. RESULTS AND DISCUSSION

A. Six zinc-blende half metals and substrates

We first confirmed our pseudopotential and LAPW predictions against available experimental and theoretical results for CrAs and CrSb. Our results are given in Table I. Using both methods, both compounds are found to be HMs with a moment of $3\mu_B$, in agreement with previous theory[16,20,28,29] and consistent with experiment.[16,17] The prediction of a CrAs equilibrium lattice constant of 5.67 Å or 5.66 Å, using LAPW or PWPP methods, respectively, is within 0.5% of the lattice constant of the substrate on which the growth was accomplished,[16] and confirms recent all-electron GGA calculations.[28] We find CrSb to be half metallic with an equilibrium lattice constant of 6.15 Å or 6.14 Å, using LAPW or PWPP methods, respectively; again within 0.5% of the lattice constant of the substrate on which the

TABLE II. Ranges of lattice constant a within ~4% of equilibrium over which half metallicity is predicted, and suggested substrates for growth. For each compound, LAPW results are listed on the first line, PWPP results on the second. Substrate lattice constants (Ref. 39) are given in parentheses.

Compound	HM a(Å)	Substrate [lattice constant (Å)]
CrP	>5.48	
	>5.47	AlP (5.53)
CrAs	>5.51	
	>5.50	GaAs (5.64), AlAs (5.62)
CrSb	>5.87 [a]	
	>5.87 [a]	AlSb (6.13), GaSb (6.12), InAs (6.04)
MnAs	>5.75	
	>5.77	InP (5.87)
MnSb	>6.06	
	>5.96	AlSb, GaSb, InAs, InSb (6.48)
MnC	<4.26	
	<4.20	Alloys of diamond (3.57), cubic SiC (4.35)

[a]Lower limit of range explored.

growth was accomplished[17] (though in this case growth was accomplished on various buffer layers, with shorter reflection high-energy electron-diffraction pattern duration for larger lattice mismatches), and confirming recent all-electron GGA results for this compound.[28]

We next searched for other Cr or Mn pnictides or carbides that might exhibit half metallicity at low (within ~4% of equilibrium) strain, and found among all possibilities just six such compounds. We confirm previous theoretical results for ZB MnAs,[17–24,27] but find ZB MnSb to be half metallic at its equilibrium lattice constant, whereas previous work[24] has found it to be only nearly so. In addition, we find two ZB compounds, CrP and MnC, to be half metallic near their respective equilibrium lattice constants. We list all six compounds in Table I, along with associated equilibrium lattice constants a_0, half metallic lattice constants a_{HM} (lattice constant nearest equilibrium at which half metallicity is predicted), density of states (DOS) at the Fermi energy for the metallic channel, gap in the insulating channel, and magnetic moment per formula unit. Based on the predicted equilibrium and half metallic lattice constants, we further suggest substrates for growth of each of the compounds with minimal strain in Table II. For each compound, we give the range of lattice constants within ~4% of equilibrium over which half metallicity is predicted, and substrates having lattice constants in the vicinity of the compound's predicted equilibrium and half metallic values.

As mentioned above, using both LAPW and PWPP methods we find ZB MnSb to be half metallic at its equilibrium lattice constant. The equilibrium lattice constant is $a_0 = 6.19$ Å, and the magnetic moment is $4\mu_B$ per f.u. This lattice constant agrees well with a previous all-electron GGA calculation[24] that obtained $a_0 = 6.166$ Å. Reference 24 reported MnSb to be close to, but not, half metallic at its equilibrium lattice constant; we find that the Fermi level is within the gap by 0.2 eV and that the lattice constant must be reduced to at least 6.09 Å before half metallicity is lost. Furthermore, we find this result to be robust with respect to the choice of computational parameters: variation with respect to basis set size, k-point mesh density, GGA functional, and core-valence energy partition were checked, and the half metallic result was obtained in all cases.

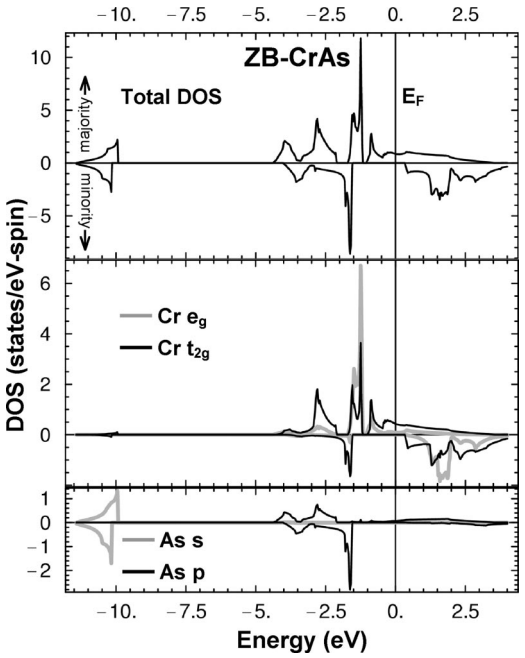

FIG. 1. Total and projected densities of states for zinc-blende CrAs. The middle and lower panels show the Cr and As contributions, respectively. Separate spin directions are plotted as indicated in the top panel.

Of particular interest in the list is MnC: unlike the pnictide compounds, we find that MnC becomes/remains half metallic with compression rather than expansion. As shown in previous investigations of transition-metal pnictides (e.g., Refs. 21, 24, 27, and 28), half metallicity is generally destroyed with compression, as valence and conduction bands are broadened, and the exchange splitting is reduced. As we discuss below, we find the nature of the half metallicity in MnC to be fundamentally different, relying rather on large bonding-antibonding splitting and moderate exchange splitting.

B. Bonding, half metallicity, and magnetic moments

To understand the bonding and half metallicity in these materials, we first consider their projected densities of states (PDOS). To clarify the differences between MnC and the rest, we compare it to one of the more studied pnictide compounds, CrAs. The results are displayed in Figs. 1 and 2. All energies are referenced to the Fermi level. A general feature of ZB structure p-d hybridization is that the e_g states are nonbonding and narrow, while the t_{2g} states mix strongly with neighboring p states and are broad.

1. CrAs

Figure 1 shows the total DOS and PDOS for CrAs at a_{HM}. It can be seen that the Cr ion is fully polarized, as is

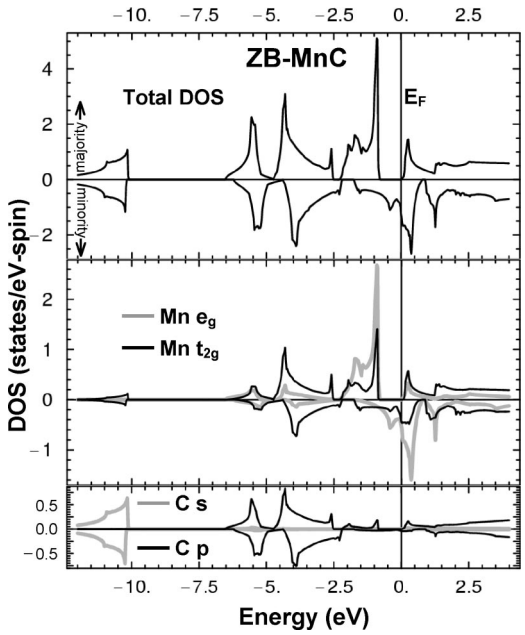

FIG. 2. Total and projected densities of states for zinc-blende MnC at its half metallic lattice constant. The larger bonding-antibonding splitting and smaller exchange splitting (middle panel) relative to CrAs and the other pnictide compounds produce a fundamentally different half metallic nature.

the case in CrO_2. The states at ~ -10 eV have anion-*s* character, and are well isolated from the bonding states. Considering the majority-spin states, the next higher energy structures between -4.5 eV and -2 eV show strong cation-t_{2g}–anion-*p* hybridization (the corresponding triply degenerate states at Γ are at -2.94 eV). These are the bonding states. The strong narrow peak at -1.3 eV has strong cation-e_g character (the doubly degenerate states at Γ are at -1.40 eV) and is associated with the nonbonding *d* states. The antibonding states form a broad structure beginning at ~ -1 eV and exhibit again mixed anion-*p* and cation-t_{2g} character. The nonbonding *d* states thus occupy the bonding-antibonding gap. To provide a measure of the *p*-*d* hybridization, we consider Γ-point energies. The unoccupied triply degenerate states at Γ are at 3.53 eV. The bonding-antibonding gap at Γ is thus 6.47 eV, which we compare to MnC below.

The minority-spin states exhibit a similar structure but are shifted up relative to the majority states by the exchange interaction. The strong peak at -1.7 eV is from the bonding *p*-*d* hybrids (with somewhat more dominant anion-*p* character than cation-*d*). The corresponding occupied triply degenerate states at Γ are at -1.66 eV. There is a separation of 6.68 eV from the next higher (unoccupied) triply degenerate states. The doubly degenerate minority states at Γ are at 1.69 eV. For all of the pnictide compounds, the antibonding states of the majority-spin channel are occupied up to E_F, leading to metallicity in that channel, while the minority channel is insulating due to the bonding-nonbonding gap.

2. MnC

The DOS for MnC at a_{HM} is shown in Fig. 2. The structures at ~ -10 eV are similar to those of CrAs (Fig. 1), i.e., essentially isolated anion-*s* states. In the region from -5.5 eV to 2.0 eV, the majority-spin DOS is also similar to that of CrAs. In MnC, however, the majority *p*-*d* hybrid antibonding states are completely above E_F. The majority *p*-*d* hybrid bonding states are centered at ~ -4.5 eV, with corresponding triply degenerate states at Γ at -5.01 eV. The corresponding triply degenerate antibonding states are at 6.79 eV. The bonding-antibonding gap at Γ is thus 11.80 eV, almost twice that of CrAs. The nonbonding *d* states contribute a strong peak at ~ -1.0 eV, with corresponding e_g states at Γ at -1.46 eV. Thus the significant differences between MnC and CrAs majority states are (i) the MnC states are broader, due to stronger *p*-*d* hybridization and greater *d*-*d* overlap (due to smaller volume[24]) and (ii) the bonding-antibonding splitting is larger in MnC, due to stronger *p*-*d* hybridization, pushing the antibonding states completely above E_F, whereas in CrAs they remain partially occupied.

There are substantial differences also in the minority states. The structure between -6.2 eV and -2.2 eV is associated with the *p*-*d* hybrid bonding states, and is broader than that in CrAs by more than 1 eV. The corresponding occupied triply degenerate states at Γ are at -4.58 eV. The Fermi energy passes through the nonbonding *d* states (with corresponding e_g states at Γ at 0.02 eV), in contrast to CrAs where the exchange splitting is sufficient to push the nonbonding states above E_F. The triply degenerate antibonding states at Γ are at 7.12 eV. Consequently, the bonding-antibonding splitting at Γ is 11.70 eV, again, almost a factor-of-2 larger than in CrAs. Thus the significant differences between MnC and CrAs minority states are (i) the MnC states are broader, due to stronger *p*-*d* hybridization and *d*-*d* overlap, and (ii) the minority nonbonding states are partially occupied in MnC, due to greater width and smaller exchange splitting, whereas in CrAs they are completely above E_F.

The origin and nature of the half metallicity in MnC is thus fundamentally different than in CrAs (and the other Cr and Mn pnictide compounds). The greater *p*-*d* hybridization and *d*-*d* overlap in MnC produces broader bands, greater bonding-antibonding splitting, and smaller exchange splitting. The net effect is to push the majority antibonding states completely above E_F and thus produce a substantial gap, making that channel insulating, while leaving the minority nonbonding states partially occupied and metallic. Thus MnC has minority spin carriers, opposite to the pnictide compounds. Furthermore, compression reinforces half metallicity in MnC by increasing the bonding-antibonding gap in the majority channel while reducing the exchange splitting, thus leaving the minority nonbonding states partially occupied. This behavior is also opposite to that in the pnictide compounds, where compression destroys half metallicity.

3. Magnetic Moments

Given the above picture of the bonding in these materials, a simple expression for their magnetic moments emerges. Reference 27 gives the relation

$$M = (Z_{tot} - 8)\mu_B \tag{1}$$

for the magnetic moment per formula unit, *M*, of half metallic zinc-blende transition-metal pnictide and chalcogenide

compounds, where Z_{tot} is the total number of valence electrons in the unit cell. The relation is predicated, however, on the assumption that the exchange splitting is sufficient to push the minority e_g states above E_F. This situation would leave the minority anion-s and p-t_{2g} hybrid states fully occupied and all higher minority states unoccupied, giving a total minority occupation of 4. Equation (1) then follows from

$$M=(N_{maj}-N_{min})\mu_B=(Z_{tot}-2N_{min})\mu_B, \qquad (2)$$

where N_{maj} (N_{min}) is the number of occupied majority (minority) states. Since the exchange splitting is not sufficient to push the minority e_g states completely above E_F in MnC, however, Eq. (1) does not hold for it. Furthermore, since in MnC the majority rather than minority channel is insulating, Eq. (2) is not readily applied. Rather, an appropriate relation for MnC, and other such compounds, follows more naturally from an equivalent expression in terms of majority occupation:

$$M=(N_{maj}-N_{min})\mu_B=(2N_{maj}-Z_{tot})\mu_B. \qquad (3)$$

In MnC, the bonding-antibonding splitting is sufficient to push the majority antibonding states completely above E_F, leaving the majority anion-s, p-t_{2g} hybrid, and e_g states fully occupied, and all higher majority states unoccupied, yielding a total majority occupation of 6. And so the appropriate relation for such compounds is

$$M=(12-Z_{tot})\mu_B. \qquad (4)$$

For MnC, $Z_{tot}=11$, and Eq. (4) predicts a moment of $1\mu_B$, in agreement with *ab initio* results. An interesting implication of Eq. (4) is that as the cation atomic number decreases, the moment should *increase*, precisely opposite to the pnictide compounds. And indeed, *ab initio* results for ZB CrC show exactly this, i.e., $M=2\mu_B$.

C. Charge Densities

In order to gain further insight into the bonding in these materials, we examine some charge densities of CrAs in a (110) plane containing a Cr-As chain. Figure 3(a) shows the charge density of an occupied triply degenerate majority state at -2.94 eV. An xy-type d-like maximum pointing from Cr toward As (e.g., around $x=0.5$, $y=0.5$) can be discerned. The maximum charge density near the Cr atom is 0.15 (since only relative values are of interest, we shall omit the units). The charge distortion that leads to a maximum along the bond (which we refer to as the bond charge) between the two atoms is evident. The maximum value in this region is 0.1. Comparing the charge distribution of a triply degenerate valence-band maximum state in GaAs [Fig. 3(b)], the shape of the density around the As atoms is similar. The maximum value in the bond charge region of GaAs is 0.13, only slightly larger than the corresponding value in CrAs. The covalent bonding in these two states seems to be comparable in the two compounds, although in CrAs the hybridization is p-d in nature whereas in GaAs it is s-p.

Figure 3(c) shows the charge density of an occupied triply degenerate minority state. The maximum of 0.07 near the Cr atom is contributed mainly by a d orbital. The maximum between the Cr and As atoms is 0.01. The charge between the two atoms in this state reflects more of an antibonding character. As shown in the PDOS (Fig. 1), the occupied minority states show somewhat more dominant anion-p than cation-d character.

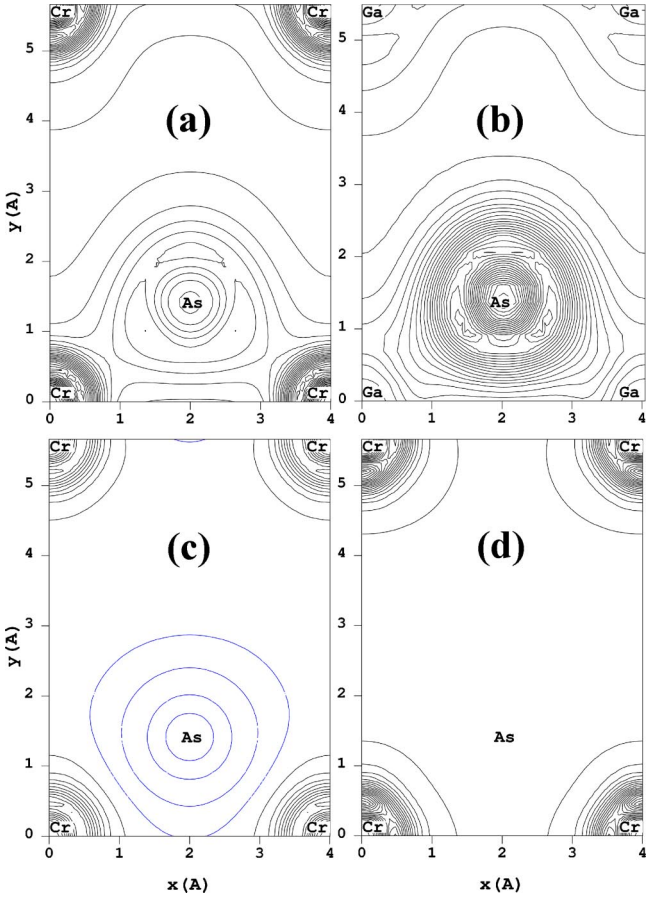

FIG. 3. Contour plots of densities of selected states in CrAs and GaAs. (a) Occupied majority-spin triply degenerate (p-t_{2g} hybrid) bonding state at Γ of CrAs. An xy-type d-like maximum pointing from Cr toward As can be discerned. The bonding character between the atoms is clearly reflected in the contour shapes. (b) Occupied p-like triply degenerate state in GaAs at Γ. Like (a), the bonding character between the atoms is evident. (c) Occupied minority-spin triply degenerate (p-t_{2g} hybrid) bonding state at Γ of CrAs. The bonding associated with these minority states is more of an antibonding character than that in (a). (d) Occupied majority-spin doubly degenerate (e_g) nonbonding state at Γ of CrAs. The state is clearly nonhybridizing in nature: the charge is completely concentrated about the Cr atoms, with no charge at the As atoms.

Figure 3(d) shows the charge density of an occupied doubly degenerate majority state. This state is clearly nonbonding in nature: the charge is completely concentrated about the Cr atoms, with no charge between atoms, and none at the As atoms.

D. Relative stability

To assess the relative stability of each compound, we consider the total energy per formula unit in the ZB structure

TABLE III. Energies per formula unit relative to the NiAs structure. For each compound and structure, the optimized lattice constant and c/a and b/a ratios are given, as appropriate. All calculations correspond to ferromagnetic ordering. Experimental lattice constants (Ref. 39) are given in parentheses.

Compound	Crystal structure	Relative energy (eV)	Lattice constant (Å)	c/a	b/a
CrP	ZB	0.839	5.42		
	NiAs	0.000	3.50	1.54	
	MnP	0.343	5.80 (5.940)	0.91	0.58
CrAs	ZB	0.768	5.66		
	NiAs	0.000	3.66	1.53	
	MnP	0.032	6.12 (6.222)	0.91	0.58
CrSb	ZB	0.940	6.14		
	NiAs	0.000	4.03 (4.108)	1.47	
MnAs	ZB	0.719	5.74		
	NiAs	0.000	3.72 (3.710)	1.49	
MnSb	ZB	0.803	6.21		
	NiAs	0.000	4.11 (4.120)	1.39	
MnC	ZB	0.555	4.39		
	NiAs	0.000	2.67	1.94	

relative to NiAs and MnP structures (Table III). Internal coordinates were taken from Ref. 39. Lattice constants were optimized for all structures, c/a ratios were optimized for NiAs structures, and c/a and b/a were optimized for MnP structures. In Table III we give for each compound and structure the optimized lattice constant a, optimized c/a and b/a as appropriate, and total energy per formula unit relative to the NiAs structure. The NiAs structure is found to be the most stable in all cases (subject to the constraint of ferromagnetic ordering employed in the present calculations). None of the compounds exhibit half metallicity in the NiAs or MnP structures.

The relative stability of the NiAs structure for the Mn pnictides is consistent with previous findings.[21,24] Quantitatively, however, for MnAs, there is some discrepancy in the literature. Using a pseudopotential LDA approach, Ref. 21 found an energy per formula unit for the ZB structure, relative to the NiAs structure, of $\sim$1.0 eV. Using an all-electron GGA approach, Ref. 24 found a value of $\sim$0.71 eV. Our ultrasoft pseudopotential GGA calculations again show excellent agreement with the all-electron calculations, with a value of 0.72 eV. Furthermore, we find a c/a ratio of 1.49, in agreement with the all-electron results. For MnSb, however, we find a significant discrepancy in the relative energy. The results of Ref. 24 show a relative ZB energy of $\sim$0.46 eV, whereas we find 0.80 eV, almost a factor-of-2 larger. However, this discrepancy may or may not be significant, since it is elsewhere noted in Ref. 24 that the energy is ''more than 0.7 eV per formula unit.''

In any case, the results demonstrate that the ZB compounds not yet grown have energies relative to the NiAs structure comparable to those compounds already grown. We emphasize, however, that the above results are only suggestive, since the true ground-state structures are in some cases considerably more complex than ferromagnetic NiAs (e.g., helimagnetic MnP in the case of CrAs), so that the results represent, strictly, merely lower bounds on instability.

IV. SUMMARY

We have applied both all-electron and pseudopotential *ab initio* methods to investigate the electronic and structural properties of ZB Mn and Cr pnictides and carbides, and found six compounds to be half metallic at or near their respective equilibrium lattice constants (Table I), making them excellent candidates for growth at low strain. Based on these findings, we further proposed substrates on which the growth may be accomplished with minimum strain (Table II). Our findings are supported by the recent successful synthesis of ZB CrAs on GaAs and ZB CrSb on GaSb, where our predicted equilibrium lattice constants are within 0.5% of the lattice constants of the substrates used. We confirmed previous theoretical results for ZB MnAs, but found ZB MnSb to be half metallic at its equilibrium lattice constant, whereas previous work has found it to be only nearly so. In addition, we found two ZB compounds, CrP and MnC, to be half metallic near their respective equilibrium lattice constants, and suggested appropriate substrates for each. Unlike the other five compounds, we found ZB MnC to become/remain half metallic with compression rather than expansion, and to exhibit metallicity in the minority- rather than majority-spin channel. Based on projected densities of states (Figs. 1 and 2) and Γ-point energies, we found that these fundamentally different properties can be understood in terms of substantially greater p-d hybridization and d-d overlap, and correspondingly larger bonding-antibonding splitting and smaller exchange splitting. Unlike the pnictide compounds, the p-d hybridization in MnC is sufficient to open up a substantial bonding-antibonding gap in the majority states, while the smaller exchange splitting brings that majority-spin gap up to, and the minority-spin e_g states down to, the Fermi energy. Based on this understanding of the bonding, we developed simple expressions for the magnetic moments in this class of compounds.

The successful synthesis and incorporation of such half metallic materials into spintronic devices holds the promise of truly on-off switching on the nanoscale, and with that, the promise of a new generation of electronic technologies. Future work will include an analysis of band structures and Fermi surfaces for these compounds in different structures, and an investigation of the critical surface and interface issues surrounding their incorporation into layered structures.

ACKNOWLEDGMENTS

This work was partially supported by NSF Grant Nos. INT-9872053 and ESC-0225007, and the Materials Research Institute at Lawrence Livermore National Laboratory (LLNL), SDSC, and NERSC. This work was performed, in part, under the auspices of the U.S. Department of Energy by the University of California, LLNL under Contract No. W-7405-Eng-48. J.E.P. thanks F.A. Reboredo and P. Söderlind for helpful discussions and independent calculations.

*Electronic address: pask1@llnl.gov

[1] G. A. Prinz, Science **282**, 1660 (1998).
[2] P. Ball, Nature (London) **404**, 918 (2000).
[3] P. Grünberg, Phys. Today **54**, 31 (2001).
[4] S. A. Wolf, D. D. Awschalom, R. A. Buhrman, J. M. Daughton, S. von Molnár, M. L. Roukes, A. Y. Chtchelkanova, and D. M. Treger, Science **294**, 1488 (2001).
[5] T. Dietl, *Diluted Magnetic Semiconductors* in *Handbook of Semiconductors* (North-Holland, New York, 1994), Vol. 3B.
[6] H. Ohno, Science **281**, 951 (1998).
[7] H. Ohno, J. Magn. Magn. Mater. **200**, 110 (1999).
[8] Y. Ohno, D. K. Young, B. Beschoten, F. Matsukura, H. Ohno, and D. Awschalom, Nature (London) **402**, 790 (1999).
[9] W. E. Pickett and J. S. Moodera, Phys. Today **54**, 39 (2001).
[10] R. A. de Groot, F. M. Mueller, P. G. van Engen, and K. H. J. Buschow, Phys. Rev. Lett. **50**, 2024 (1983).
[11] J.-H. Park, E. Vescovo, H.-J. Kim, C. Kwon, R. Ramesh, and T. Venkatesan, Nature (London) **392**, 794 (1998).
[12] K. Schwarz, J. Phys. F: Met. Phys. **16**, L211 (1986).
[13] K. P. Kämper, W. Schmitt, G. Güntherodt, R. J. Gambino, and R. Ruf, Phys. Rev. Lett. **59**, 2788 (1987).
[14] R. J. Soulen, Jr., J. M. Byers, M. S. Osofsky, B. Nadgorny, T. Ambrose, S. F. Cheng, P. R. Broussard, C. T. Tanaka, J. Nowak, J. S. Moodera, A. Barry, and J. M. D. Coey, Science **282**, 85 (1998).
[15] D. Ristoiu, J. P. Nozières, C. N. Borca, B. Borca, and P. A. Dowben, Appl. Phys. Lett. **76**, 2349 (2000).
[16] H. Akinaga, T. Manago, and M. Shirai, Jpn. J. Appl. Phys., Part 2 **39**, L1118 (2000).
[17] J. H. Zhao, F. Matsukura, T. Takamura, E. Abe, D. Chiba, and H. Ohno, Appl. Phys. Lett. **79**, 2776 (2001).
[18] M. Shirai, T. Ogawa, I. Kitagawa, and N. Suzuki, J. Magn. Magn. Mater. **177–181**, 1383 (1998).
[19] T. Ogawa, M. Shirai, N. Suzuki, and I. Kitagawa, J. Magn. Magn. Mater. **196–197**, 428 (1999).
[20] M. Shirai, Physica E (Amsterdam) **10**, 143 (2001).
[21] S. Sanvito and N. A. Hill, Phys. Rev. B **62**, 15 553 (2000).
[22] S. Sanvito, P. Ordejón, and N. A. Hill, Phys. Rev. B **63**, 165206 (2001).
[23] S. Sanvito, G. Theurich, and N. A. Hill, J. Supercond. **15**, 85 (2002).
[24] A. Continenza, S. Picozzi, W. T. Geng, and A. J. Freeman, Phys. Rev. B **64**, 085204 (2001).
[25] Y.-J. Zhao, W. T. Geng, A. J. Freeman, and B. Delley, Phys. Rev. B **65**, 113202 (2002).
[26] I. Galanakis, Phys. Rev. B **66**, 012406 (2002).
[27] I. Galanakis and P. Mavropoulos, Phys. Rev. B **67**, 104417 (2003).
[28] B.-G. Liu, cond-mat/0206485 (unpublished).
[29] A. Sakuma, J. Phys. Soc. Jpn. **71**, 2534 (2002).
[30] W. Kohn and L. J. Sham, Phys. Rev. **140**, A1133 (1965).
[31] G. Kresse and J. Hafner, Phys. Rev. B **47**, 558 (1993); **49**, 14 251 (1994).
[32] G. Kresse and J. Hafner, J. Phys.: Condens. Matter **6**, 8245 (1994).
[33] G. Kresse and J. Furthmüller, Phys. Rev. B **54**, 11 169 (1996).
[34] W. E. Pickett, Comput. Phys. Rep. **9**, 115 (1989).
[35] P. Blaha, K. Schwarz, and J. Luitz, WIEN97, *A Full Potential Linearized Augmented Plane Wave Package for Calculating Crystal Properties* (Karlheinz Schwarz, Technische Universität Wien, Austria, 1999). ISBN 3-9501031-0-4.
[36] D. J. Singh, *Planewaves, Pseudopotentials, and the LAPW Method* (Kluwer Academic, Boston, 1994).
[37] J. P. Perdew, J. A. Chevary, S. H. Vosko, K. A. Jackson, M. R. Pederson, and C. Fiolhais, Phys. Rev. B **46**, 6671 (1992).
[38] J. P. Perdew, K. Burke, and M. Ernzerhof, Phys. Rev. Lett. **77**, 3865 (1996).
[39] R. W. G. Wyckoff, *Crystal Structures*, 2nd ed. (Interscience, New York, 1963), Vol. 1.